



Contrasting features of monsoon convection over land and sea in the west coast of peninsular India as revealed by S-band radar

S. B. Morwal¹ · B. Padmakumari² · R. S. Maheskumar³ · K. S. Hosalikar⁴ · K. C. Sai Krishnan⁵ · S. G. Narkhedkar⁶ · G. Pandithurai² · J. R. Kulkarni⁷

Received: 2 November 2021 / Accepted: 24 August 2022 / Published online: 31 August 2022
© The Author(s), under exclusive licence to Springer-Verlag GmbH Austria, part of Springer Nature 2022

Abstract

Monsoon convection characteristics over land and sea within 150 km of the west coast of India are studied using coastal Mumbai S-band radar. The intraseasonal and interannual monsoon variabilities in cloud characteristics are investigated for the contrasting monsoon seasons of 2013 and 2014. The cloud characteristics studied are frequency of occurrences, cloud top height (CTH), longitudinal distribution, diurnal variation, and scale-wise distribution of cloud cells. The number of cloud cells is about four times higher over land than over sea. The maximum frequency of CTH is found in the cumulus category (3–4 km). The mean CTH varies from 4.49–5.44 km. No significant difference between the CTH over the land and sea regions is found. The contribution of congestus to total cloud cells is found maximum over both land and sea. The longitudinal variation of cloud frequency shows maximum frequency at a distance of 50–60 km from the location of radar over both sea and land. The maximum over the land region is the new feature revealed in the analysis. The diurnal variation of clouds shows a broad structure with maximum in the local noon and minimum in the morning hours. The mean duration of the clouds is 40–44 min both over land and sea. The contribution by the mesoscale convective system (MCS) is dominant (57–63%). The study of cloud distribution over land and sea over the west coast of India using radar data is the first of its kind and has brought out detailed structure of cloud distribution with time and space.

1 Introduction

The west coast of peninsular India receives high summer monsoon (June–September) rainfall (> than 200 cm) (Rao 1976). This quantity of rainfall is more than two and half times of all India mean monsoon rainfall which is 84 cm (Parthasarathy et al. 1995). The paper by Maheskumar et al. (2014) (and references therein) gives account of studies done in understanding the high rainfall over the region. The roles

of dynamic, thermodynamic, and microphysical processes responsible for occurrences of high rainfalls have been discussed in that paper. The mechanism leading to high seasonal rainfall has been explained following different steps (Figs. 1, 2, 3, 4, 5, 6 and 7).

Grossman and Durran (1984) showed that the low-level monsoon southwesterly winds over the Arabian Sea (AS) experience the impact of west coast mountains (referred as Western Ghats: WG) in decelerating the flow resulting into development of offshore convergence zone. The low-level wind convergence generates large-scale upward motion. The monsoon flow approaching the west coast is convectively unstable. These conditions are suitable for the development of spectrum of clouds ranging from shallow to deep depending upon the offshore distance from the west coast. Grossman and Durran (1984), using the aircraft, radar, and satellite data, showed (Fig. 8a in their paper) existence of deep convective clouds off the coast within distance of 200 km. The prevalence of deep convection off the coast has been shown by Roca and Ramanathan (2000) and Francis and Gadgil (2006) using satellite data. The shallow clouds prevailed further west from the coast. Medina et al. (2010)

✉ B. Padmakumari
padma@tropmet.res.in

¹ Vanashree Apartment, Bavdhan, Pune, India
² Indian Institute of Tropical Meteorology, Ministry of Earth Sciences, Pune, India
³ Ministry of Earth Sciences, New Delhi, India
⁴ India Meteorological Department, Pune, India
⁵ Regional Meteorological Centre, New Delhi, India
⁶ Safalya, Swami Vivekananda Nagar, Pune, India
⁷ Rajyog Society, Baner, Pune, India

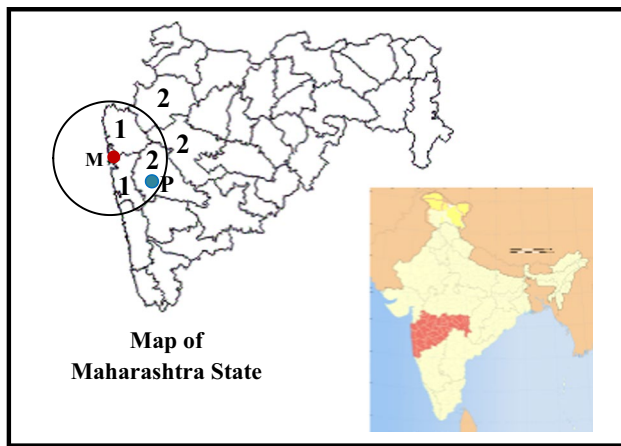


Fig. 1 Map of Maharashtra State showing the location of the S-band radar (red solid circle) at Mumbai (M). The study region using radar data is shown by black circle. The location of Pune (P) is shown by blue solid circle. The districts in (within the radius of 150 km) subdivisions Konkan & Goa and Madhya Maharashtra are indicated by numbers 1 and 2, respectively. Inset is map of India showing the location of Maharashtra state with red shade

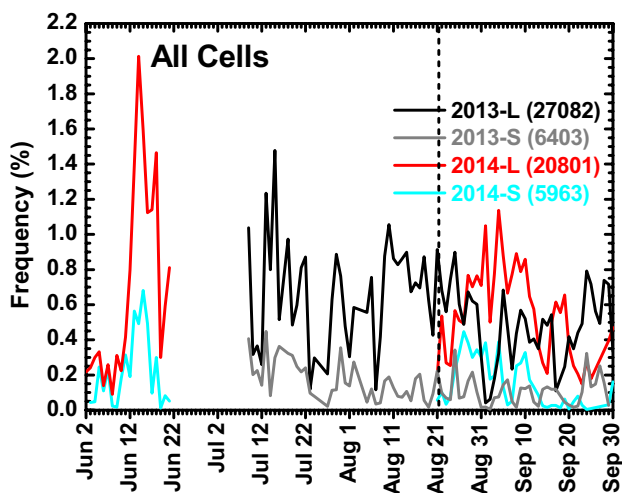


Fig. 2 Frequency distribution of all cells (normalized by 60,249 = sum of cells over land and Sea during 2013 and 2014) during summer monsoon seasons of 2013 (9 July to 30 September) and 2014 (2–21 June and 21 August – 30 September) over the land and sea regions. The vertical dashed black line indicates the common period for which the data is available during both the years 2013 and 2014

showed that with aging and due to wind shear, the deep convective clouds transform into stratiform types. These convective and stratiform clouds travel towards the coast and produce high rainfall over the coast.

Weather radar provides spatio-temporal variability of convection with high resolution. Using Tropical Rainfall Measurement Mission (TRMM) radar reflectivity data, three types of clouds have been categorized by Houze

et al. (2007), Romatschke et al. (2010), and Romatschke and Houze (2011). These are (i) “deep convective cores” (contiguous 3-D convective echo with reflectivity > 40 dBZ extending up to > 10 km in height), (ii) “wide convective cores” (contiguous convective echo with reflectivity > 40 dBZ over a horizontal area > 1000 km²), and (iii) “broad stratiform regions” (stratiform echo contiguous over an area > 50,000 km²). Houze (2012) showed the climatological distribution of frequency of occurrences of these three types of cloud systems over AS. The majority of cloud types over AS were found to be wide convective cores and broad stratiform regions with zero frequency of deep convective cores. As shown by Houze (1997), the microphysical growth processes are different in convective and stratiform clouds. Radar data can be found useful in improving the accuracy of the numerical weather prediction if the data pertaining to spatial distribution of convection is properly ingested in the data assimilations (Osuri et al. 2015).

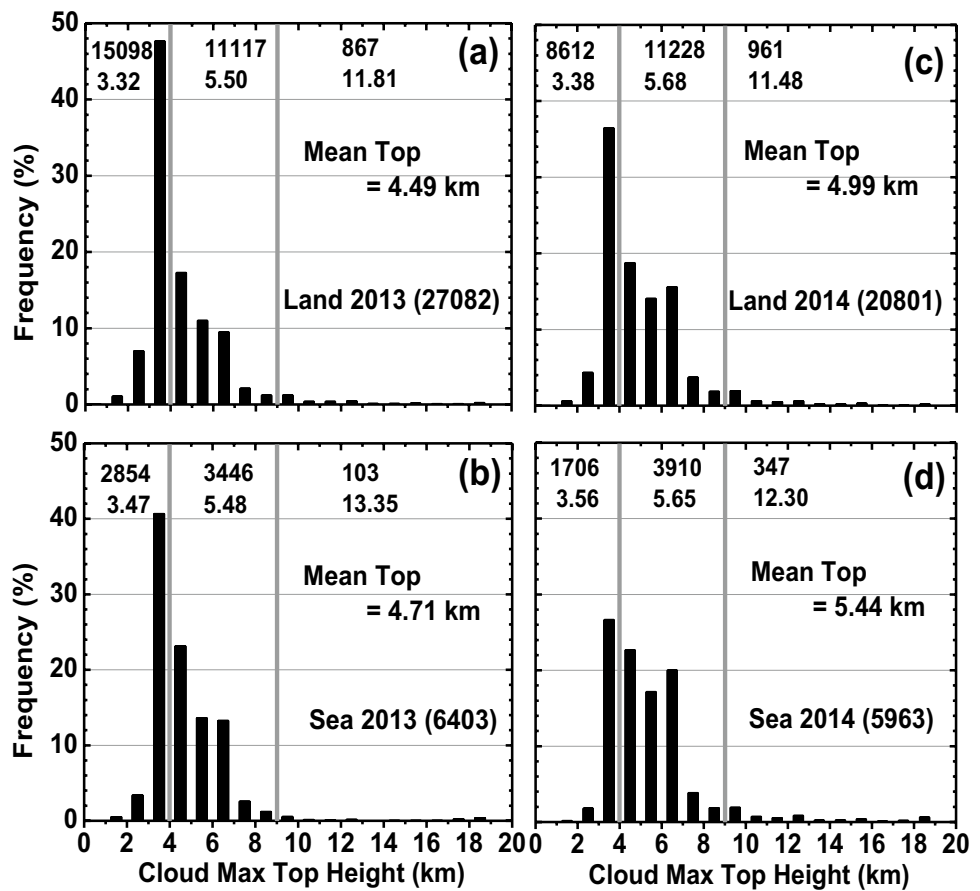
Three dimensional characteristics of the precipitating clouds during Indian summer monsoon have been investigated by Shailendra Kumar (2016, 2017) using 10 years of Tropical Rainfall Measuring Mission Precipitation Radar (TRMM PR) and studied the properties of clouds over Indian land mass and oceanic areas. They observed intense cloud systems over land compared to oceanic areas and also showed that over the Western Ghat mountains ~ 13% of the cells have their tops below the freezing level. In their another study, Shailendra Kumar and Bhat (2017) also showed that Western Ghat mountains contain the highest fraction of shallow echo-top clouds.

The study of the monsoonal cloud systems using radar data has been done by Sindhu and Bhat (2018). In this study, interactions between mesoscale convective systems and individual clouds were examined using the data of IMD Doppler weather radars located at Hyderabad, Kolkata, Nagpur, and Patiala. The study brought out that average storm area in monsoonal cloud systems varies from ~20 to 170 km² while storm height mostly lies between 6 and 10 km.

The seasonal characteristics of the cloud systems over Indian subcontinent have been studied by Sindhu and Bhat (2021). In their study, pre-monsoon and monsoon season characteristics of clouds were studied using radar data at Lucknow, Bhopal, Patna, and Nagpur. The characteristic values of different cloud parameters estimated were speed of propagation of cloud system (5–60 km per hour), life time (0.3–3 h), volume (8–1600 km³), echo top height (2–14 km), and thickness (0.5–6 km), respectively. As per authors’ opinion, these cloud characteristic values are important for the numerical short range weather forecasting and for development of cloud parametrization schemes.

The studies regarding spatio-temporal variability of convection at a high resolution in space and time over the west coast of India are lacking. This has motivated

Fig. 3 Frequency distribution of cloud maximum top height (CTH, %) using radar during the summer monsoon season for 2013 over (a) land and (b) Sea region and 2014 over (c) land and (d) Sea region. The vertical gray lines delineate the cloud categories of cumulus (CTH: 0–4 km), congestus (CTH: 4–9 km) and cumulonimbus (CTH: > 9 km). The numbers in each plot represent the number of clouds (line 1) and average CTH in that cloud category (line 2)



us to take up the study of the convection over the west coast of India using Mumbai radar (site location given in data section) reflectivity data. The land-sea contrast influences the distribution of convection. Mumbai radar data is useful in examining the differences between the convection over sea and land, if any, as half the coverage area of the radar is over the sea and remaining half is over the land. In each monsoon season, very heavy rainfall events occur over Mumbai on a number of occasions. These cause flash floods, inconveniences to residents, paralyzing transport system, and many sufferings to common people. The mechanism of very heavy rainfalls has been studied using the radar data.

The specific objectives of the paper are to study (1) cloud cell distribution in different monsoon seasons and (2) their contrasting features over land and sea. The paper is organized as follows: The description of radar, its data, and the prevailing meteorological conditions are given in Sect. 2. Section 3 describes the distribution of the cells. The mechanism of high rainfall over the coast and adjacent land region as emerged from the analysis is described in Sect. 4. Conclusions are given in Sect. 5.

2 Data and meteorological conditions

Mumbai is the financial capital of India, located on the west coast of India in the state of Maharashtra (Fig. 1 inset). S-band Doppler radar is operated continuously by India Meteorological Department (IMD) in south Mumbai located at Navy Nagar, Colaba (18.90° N, 72.81° E, 4 m amsl) since October 2010. Colaba is located on the coast of the AS (Fig. 1 red solid circle and symbol M). The radar is operated in surveillance mode. It collects the cloud reflectivity data in 3-dimensional volume scans at an interval of ~ 11 min. The data are collected at 10 vertical levels (0.2, 1, 2, 3, 4.5, 6, 9, 12, 16, and 21 deg). The range of the radar is 250 km. The technical details of the radar are given in Table 1.

Radar reflectivity data over the circular area of 150 km radius (shown by black circle in Fig. 1) has been used in the study. This areal limit has been used in the previous studies (Goudenhoofd et al. 2010; Kumar et al. 2013a, b; May and Ballinger 2007; Morwal et al. 2016, 2017) as after 150 km the lowest radar beam goes more than 2 km

Fig. 4 Cumulative frequency distribution of cloud maximum top height (CTH, km) plotted in log-probability format during the summer monsoon season for 2013 over (a) land and (b) sea region and 2014 over (c) land and (d) sea region. The straight line in each plot represents the log-normal cumulative distribution fitted with the mean (Avg) and standard deviation (Std) of the CTHs as shown in all the plots

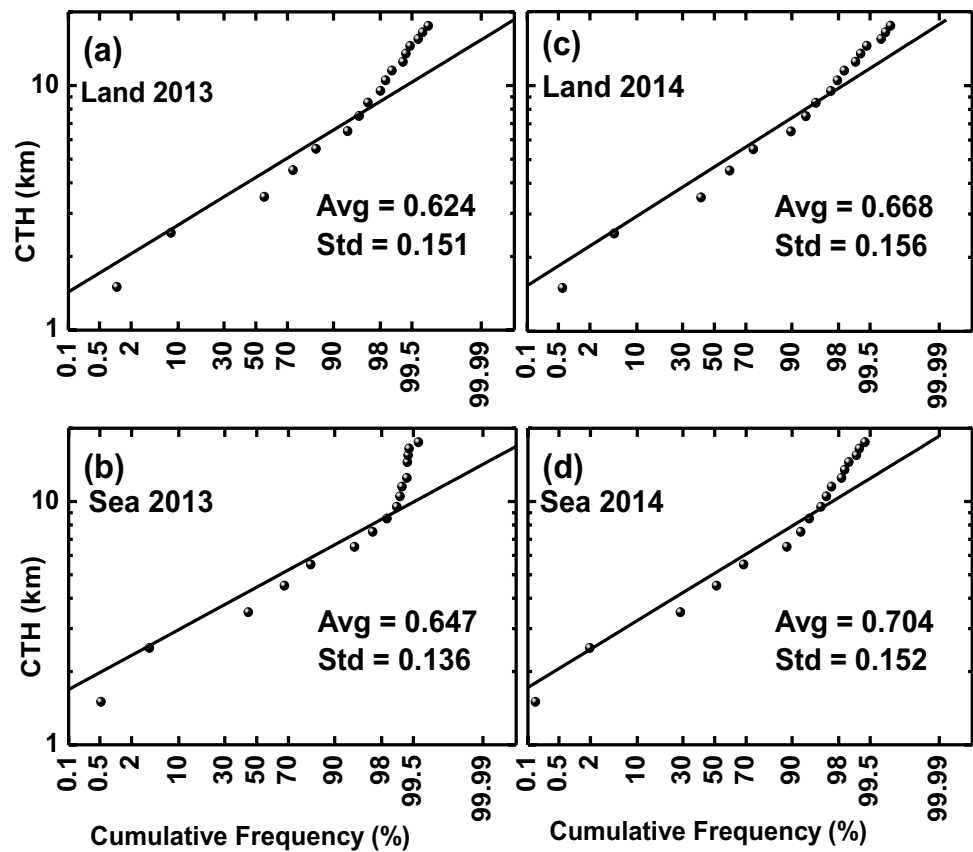
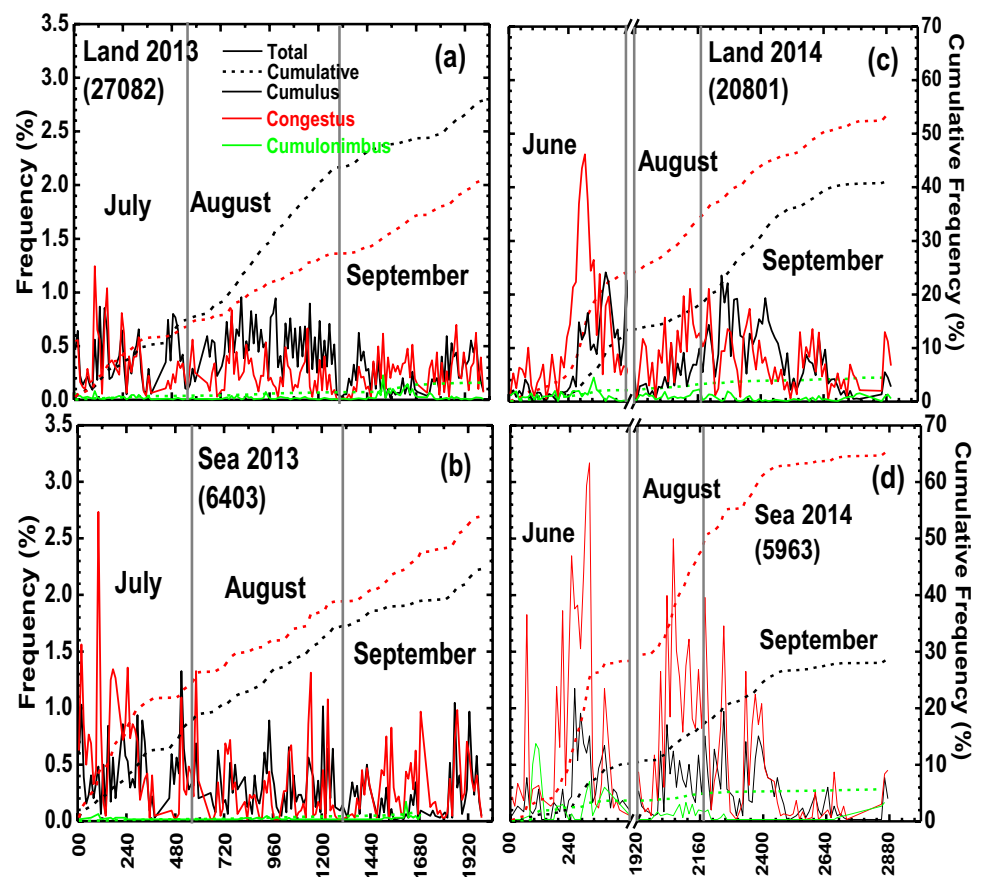


Fig. 5 Twelve-hourly time series of frequency of clouds (% , normalized w.r.t. total number of clouds shown by solid lines) along with the cumulative frequency distribution (% , dashed line) of cumulus (black lines), congestus (red lines) and cumulonimbus (green lines) clouds during the summer monsoon season for 2013 over (a) land and (b) sea region, and for 2014 over (c) land and (d) sea region



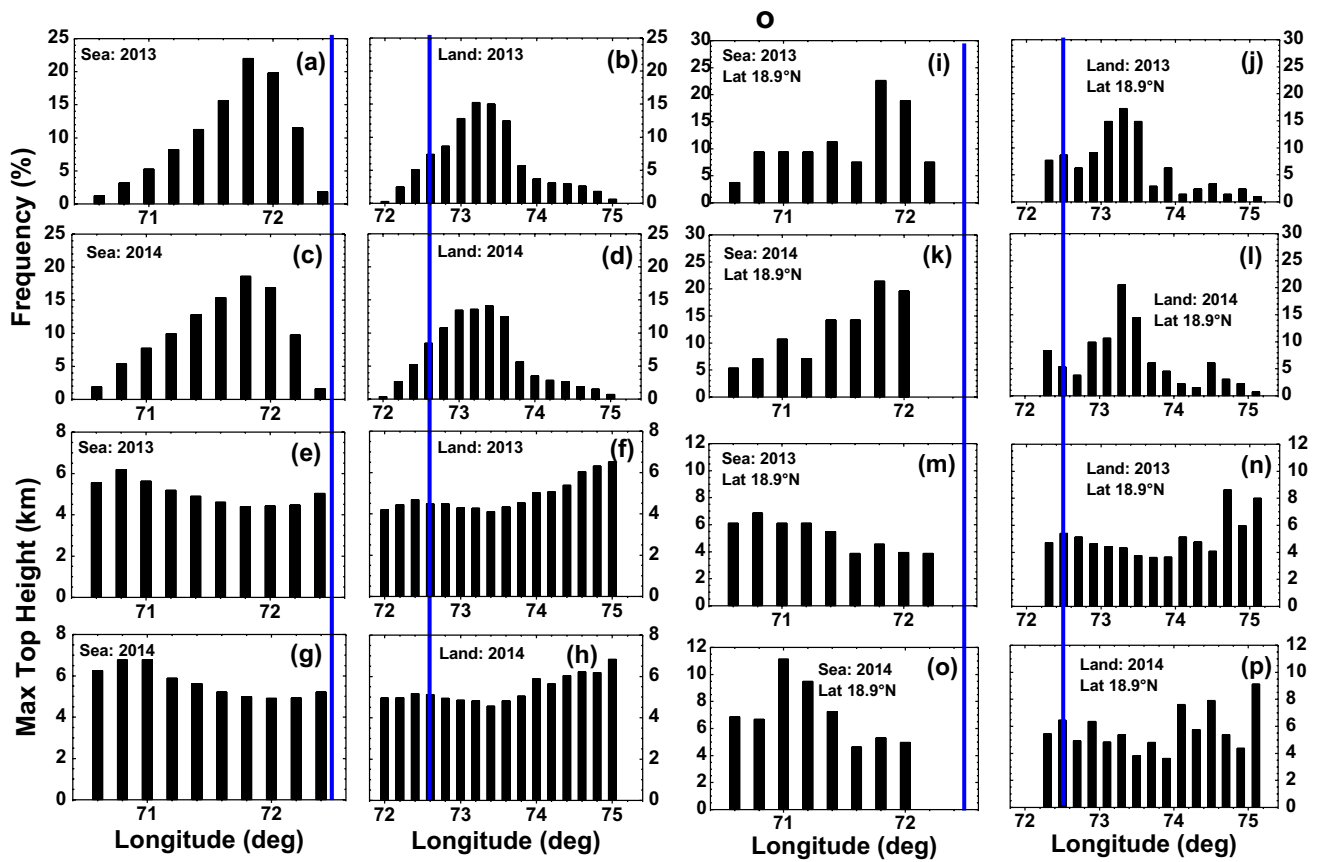


Fig. 6 Longitudinal variation of frequency of occurrence of cloud cells (%) and maximum cloud top height (km) during the summer monsoon season for 2013 and 2014 (1) all observations: over sea (a,

c and e, g) and land (b, d and f, h) and (2) at radar latitude (18.9°N): over sea (i, k and m, o) and land (j, l and n, p). Vertical blue line indicates the radar longitude

above the ground and beam spreads vertically to a larger cross-section. This horizontal limit of 150 km is used to get the unambiguous count of the reflectivity cells. Hereafter, this is defined as “study area.” The radar data has been analyzed using the TITAN (Thunderstorm Identification, Tracking, Analysis and Nowcasting) software (Dixon and Wiener 1993) to identify the cloud cells from the reflectivity Cartesian data. The cell is defined as the three-dimensional region which exceeds the reflectivity of 5 dBZ in the volume Cartesian data at least for two consecutive time steps (Dixon and Wiener 1993; May and Ballinger 2007; Morwal et al. 2016, 2017). The criteria adopted to select the cells in this study are similar to those followed in the past studies (Kumar et al. 2013a, b; May and Ballinger 2007). The criteria are (i) range radius ≤ 150 km, (ii) $19 \text{ km}^2 < \text{cell Area} < 71,000 \text{ km}^2$, and (iii) Maximum cell top height < 18.6 km.

The period of the study is the summer monsoon seasons (June–September: JJAS) of 2013 and 2014. During the season 2013, the reflectivity data are available from 9 July to 30 September. In the season 2014, the radar data are available for the periods 2 – 21 June and 21 August—30 September

and there is a gap from 22 June–20 August. The period excluding gaps is referred to as “the study period.” Since the radar is situated on the AS coast, it covers both the sea and land regions. Therefore, the study area is divided into land and sea regions to compare the convection characteristics over both areas. For meteorological purposes, India is divided into 36 subdivisions. Over the land, the 150 km radius from the radar center covers parts of Konkan & Goa and Madhya Maharashtra subdivisions (Fig. 1).

The seasonal rainfalls in the summer monsoon seasons of 2013 and 2014 over the country were 106% and 88%, respectively of its long period average (LPA). LPA of all India and subdivisional monsoon rainfall have been estimated as the average rainfall for the period of 1871–2016 (Kothawale and Rajeevan 2017). As per IMD definition, all India monsoon is categorized as normal if the all India monsoon rainfall in the year lies within + or – of 10% of LPA of monsoon rainfall. For the sub-divisional case, if the monsoon rainfall lies within + or – 10 % of the LPA of the subdivision, then it is termed as normal rainfall of the subdivision. Thus, over the country, the monsoon seasons 2013 and 2014 are categorized as normal and below

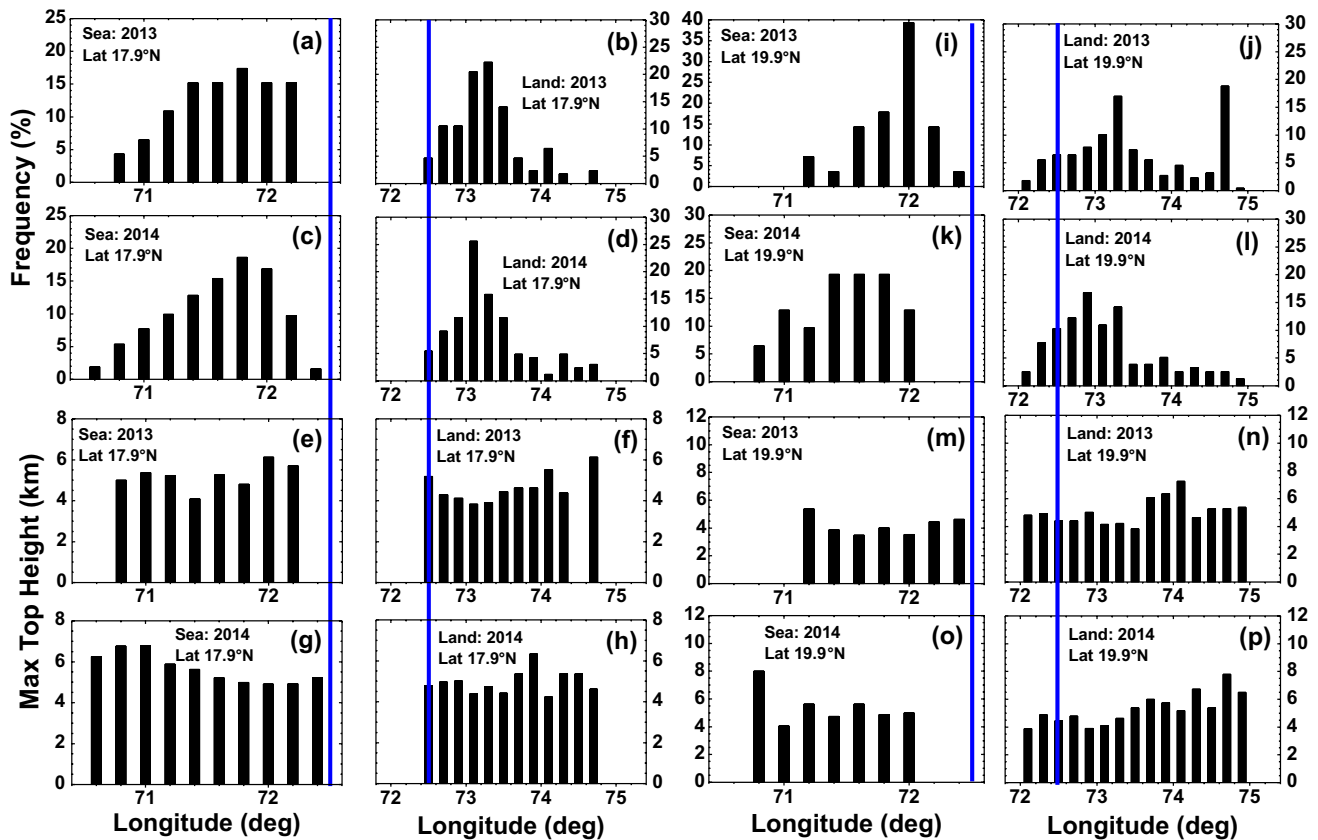


Fig. 7 Longitudinal variation of frequency of occurrence of cloud cells (%) and maximum cloud top height (km) during the summer monsoon season for 2013 and 2014 (1) at latitude 17.9° N: over Sea

(a, c and e, g) and land (b, d and f, h) and (2) at latitude 19.9° N: over Sea (i, k and m, o) and land (j, l and n, p). Vertical blue line indicates the radar longitude

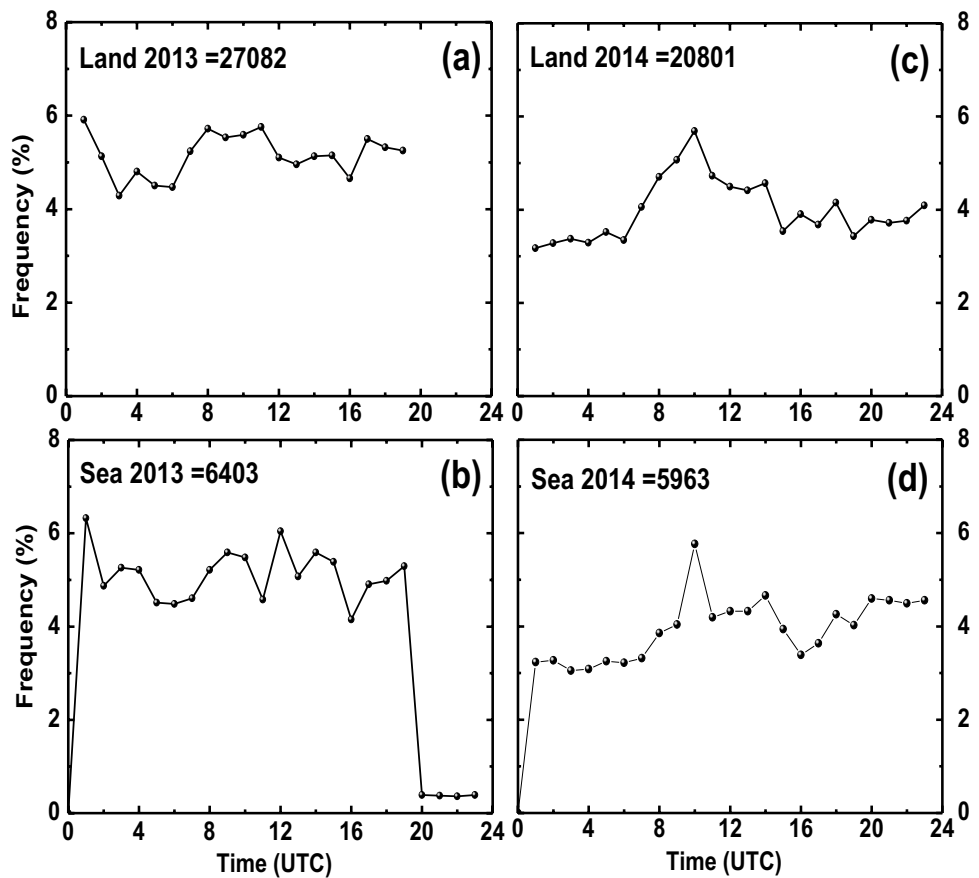
normal monsoon years, respectively. The cities of Mumbai and Pune (18.52° N, 73.86° E, 552 m amsl, shown by blue solid circle with symbol P) are located in the Konkan & Goa and Madhya Maharashtra meteorological subdivisions, respectively (which are indicated by number 1 and 2, respectively in Fig. 1). Month-wise rainfall departures over these subdivisions in the summer monsoon seasons of 2013 and 2014 from their LPA (%) are given in Table 2. In the year 2013, the rainfall departures were positive in the months of June, July, and September and negative in the month of August over both the subdivisions. For the season 2013, the departures were $\sim 20\text{--}21\%$ over both the subdivisions indicating that it was excess monsoon year as far as the rainfall activity over these two subdivisions are concerned (Fig. 6 of Weather in India 2014). The rainfall departures in the season 2014 were negative in the months of June and August for Konkan & Goa subdivision and in the months of June and September for Madhya Maharashtra subdivision. The departures for the seasons 2014 are $\sim -6\%$ for both the subdivisions indicating normal rainfall, and hence, 2014 is a normal monsoon year for these two subdivisions (Fig. 6 of Weather in India

2015). The positive departures (active period) and negative departures (break period) in the daily rainfall time series are intraseasonal features of monsoon rainfall. The rainfalls in the two years are similar to typical features of interannual variability of monsoon rainfall. Though the study is for two years, it covers typical intraseasonal and interannual monsoon variability, and therefore, it is representative of climatic feature of the monsoon variability. Such an approach has been adopted in our previous papers (Morwal et al. 2016, 2017).

3 Statistical cloud characteristics using radar

Here an attempt has been made to examine the storms (hereafter called as cloud or cell) characteristics, identified using the TITAN software, over both the sea and land regions. The cloud characteristics include distribution of cloud cells, cloud maximum top heights (CTH), cloud duration, and spatial distribution of clouds based on scale analysis.

Fig. 8 Diurnal variation of number of clouds (%) during the summer monsoon seasons of 2013 over (a) land and (b) sea region and 2014 over (c) land and (d) sea region



3.1 Distribution of cloud cells

The time series of frequency of occurrence (%) of cloud cells is given in Fig. 2 over the land (L) and sea (S) regions for the summer monsoon seasons of 2013 (black and grey) and 2014 (red and cyan). The total number of cloud cells for all categories is indicated in the legend. There are 60,249 cloud cells altogether during both the years. The total number of cloud cells during the summer monsoon seasons of 2013 and 2014 are nearly 4 times higher over the land regions (2013: 44.95% and 2014: 34.52%) as compared to that over the sea (2013: 10.63% and 2014: 9.90%) region. The total number of cloud cells available on daily scale are normalized by total number of 60,249 cloud cells (sum of all cloud cells during 2013 and 2014) in order to compare the frequency of occurrences of cloud cells during both the years over land and sea regions on daily time scale. In the monsoon season 2013, the radar reflectivity data is available from 9th July to 30th September, whereas in the monsoon season 2014 the radar reflectivity data is available from 2 June to 30th September with a gap in the data from 22 June to 20 August. It is seen from the daily time series that even though the frequency of occurrence of cloud cells over the land region is much higher as compared to that over the sea regions, the daily variation is similar. The period 21 August to 30 September (marked

by dashed vertical lines in Fig. 2) is the common period in which the radar reflectivity data are available in both years. The total number of cloud cells during this period (30,347) is more than half of the total number of cloud cells (60,249). In this common period, the frequency of occurrence of cloud cells is higher during the period 27 Aug to 12 Sep over the land/sea regions during 2014 in comparison to that of 2013, respectively.

3.2 Distribution of CTH

Radar cloud/echo top height is one of the important factors to evaluate the intensity of convective clouds. The cloud/echo top height is the maximum height of the minimum detectable reflectivity (Donaldson 1964). Here we have considered the reflectivity of 5 dBZ to detect the CTHs for studying the vertical structure of the clouds. The CTH has been studied by Houze and Cheng (1977), Lo´pez (1977), Johnson et al. (1999), DeMott and Rutledge (1998), Kokhanovsky et al. (2007), and Bhat and Kumar (2015). By following the method of Johnson et al. (1999) and that of Morwal et al. (2016, 2017), the clouds are categorized into three categories based on the CTH as (i) shallow cumulus clouds ($0 < CTH \leq 4$ km), (ii) congestus clouds

Table 1 Technical specification of the S-band Doppler weather radar located at India Meteorological Department, Colaba, Mumbai, India

Place of installation	NOFRA, Colaba, Mumbai, INDIA	Latitude: 18° 54' 04"N, Longitude: 72° 48' 32"E Height above msl: 3.220 m Height of Bldg: 59.65 m
Radome (Metstar)	Material Diameter Wind speeds	Foam sandwich rigid, spherical 11.8 m truncated at 87% 250 Kmph steady, gusting to 300 Kmph
Antenna	Shape Diameter/beam width Polarization Steer ability Rotation Rate	Prime focus Parabolic dish 9 m / 0.95 deg Dual polarization for radar polarimetry 360° in Azimuth, -1 to +90 deg in elevation Up to 6 RPM
Transmitter (Coherent – Klystron)	Peak power Pulse width PRF Modulator	1.0 MW 0.5 to 4 μ sec (selectable) 250 to 2000 Hz (selectable) Solid state modulator (forced air cooled)
Receiver (Coherent)	Dynamic range Noise figure IF	95 dB 3 dB 30 MHz
Servo System	Pedestal type Azimuth travel Elevation travel Acceleration in Az and El Motors used	Elevation over Azimuth Continuous (0 to 360 deg) and 6 RPM -1 to 90 deg and 10 deg/sec Up to 10 deg/sec ² Koll–Morgan Motor MH – 627E (12.65 HP)
Computer System	Operating system Data storage	Linux/Windows Workstations Storage server of capacity 2 TB (Max)

Table 2 Monthwise rainfall departure from its long period average (LPA, %) during the summer monsoon seasons (June–September) of 2013 and 2014 for the subdivisions of Konkan and Goa, Madhya Maharashtra and country India

Month	Departure from LPA (%) for 2013			Departure from LPA (%) for 2014		
	Konkan and Goa	Madhya Maharashtra	Country (India)	Konkan and Goa	Madhya Maharashtra	Country (India)
J: June	53	46	34	-63	-70	-42
J: July	40	29	7	22	15	-10
A: August	-32	-22	-2	-8	27	-9
S: September	2	38	-12	27	-21	8
JJAS: June–September	20	21	6	-6	-6	-12

(4 km < CTH ≤ 9 km), and (iii) cumulonimbus clouds (CTH > 9 km).

The frequency distribution of the CTH during 2013 and 2014 over land and sea regions is shown in Fig. 3a–d. The maximum CTH is 18.6 km. The vertical gray lines in each plot denote the partition between the different cloud categories as defined above. Thus, the first 4 CTH classes belong to cumulus, the next 5 classes belong to congestus, and all remaining classes belong to the cumulonimbus category. The number of clouds present in each cloud category is

indicated (Top value) along with the average value of CTH in that category (bottom value). The total number of clouds over the land/sea regions during the study period of 2013 and 2014 are 27,082/6403 and 20,801/5963, respectively. The frequency distribution of CTH is positively skewed in all the plots. This is similar to the one observed by Lo'pez (1977) and Morwal et al. (2016). In all the plots, the maximum frequency of occurrence is in the CTH class 3–4 km which is in the cumulus category, the second maxima is seen in the CTH class 4–5 km which is in the congestus

category, and thereafter the frequency decreases continuously in cumulonimbus category with increasing CTH with maximum in the 9–10-km class. The mean CTH varies from 4.49 to 5.44 km and CTHs are slightly higher over the sea region (4.71 and 5.44 km) as compared to the land region (4.49, 4.99 km) in both years; however, the difference is not statistically significant. This is also applicable to all the cloud categories. These values of CTH are comparable to that reported over the sea regions (over the northwestern Atlantic Ocean (~4.91 km) (Lo'pez 1976) and over GATE region (~4.8 km) (Houze and Cheng 1977). However, these values of CTH are lower than those observed over land regions: over the rain-shadow regions of north central peninsular India (~7.5 km) during withdrawal and post-withdrawal period (Morwal et al. 2016), over the rain-shadow region of peninsular India (~8.2 km over Baramati and Shegaon, Morwal et al. 2017), over Darwin, Australia (~8 km), during wet season (Kumar et al. 2013a) and over the Tucson, Arizona, semi-arid region (~7.1 km) (Braham 1958). These values of CTH are comparable to that reported by Kokhanovsky et al. (2007) as the global value of CTH (~6 km). This shows that there is no significant difference between the CTH over the land and sea regions within the radius of 150 km from the location of the radar (and clouds show marine characteristics). This indicates that the clouds originated over the sea are not modified by the presence of land for short inland travels.

Cumulative frequency distributions of CTH over land/sea regions during 2013 and 2014 seasons are shown in Fig. 4a–d in log-probability format. The lognormal distribution of the CTH is fitted by considering the logarithms of the CTH with average (Avg) and standard deviation (Std) as given in each individual plots. This is represented by a straight line in each plot. The dots represent the cumulative frequencies of CTH (%). It is seen that the observed cumulative frequency of CTH follows the lognormal fit line up to ~10–11 km height and include >95% but less than 99% of the observations. After that, there is a deviation from the lognormal fit line in the higher height range. Lo'pez (1977), Houze and Cheng (1977), and Morwal et al. (2016, 2017) have also observed the deviation in the higher height range of the CTH which they have attributed to the truncated lognormal distribution.

It is interesting to examine the 12-hourly variation of the frequency (%), and cumulative frequency (%) of the cumulus, congestus, and cumulonimbus clouds over land and sea regions during the summer monsoon season. The frequency (%), normalized w.r.t. total number of clouds given in bracket in each figure and shown by solid line) and cumulative frequency (%), dashed lines) are shown in Fig. 5a–d over the land/sea region during summer monsoon season of 2013 and 2014. Distribution of cumulus is shown by black color, congestus by red color, and that of cumulonimbus by green

color. The vertical gray lines separate the months. The rainfall departures (%) from the long period average for the subdivisions of (i) Konkan & Goa, (ii) Madhya Maharashtra, and for the country as a whole during the summer monsoon months are shown in Table 2. These two subdivisions are considered because the land area within the radius of 150 km mostly belongs to these two subdivisions. From Table 2, it is seen that in June, July, September, and JJAS rainfalls are above normal in the monsoon season 2013 over Konkan & Goa and Madhya Maharashtra subdivisions. In the monsoon season 2014, over these two subdivisions, rainfall departures in the month of June were below normal, in July, the rainfall departure over Konkan & Goa subdivision was in excess category, but over Madhya Maharashtra, the rainfall departure was in normal category. In the month of August 2014, rainfall departure over Konkan & Goa subdivision was in normal category and over Madhya Maharashtra in excess category. When the entire JJAS season is considered, over Konkan & Goa and Madhya Maharashtra subdivisions, departures of rainfalls in 2014 season were in normal category, and in 2013 in excess category.

From Fig. 5a, c, it is seen that the contributions from the cumulonimbus clouds to total cloud frequency count given in bracket in each figure are very low compared to cumulus and congestus over the land region. In the monsoon season 2014, over the land region (Fig. 5c), the contributions by congestus clouds are more than those of cumulus in the months of June, August in the later parts of the September, and over the sea, the contributions by congestus (Fig. 5d) are higher than cumulus in all the 3 months. In the monsoon season 2013, the contributions by congestus over sea (Fig. 5b) are more than those of cumulus, but over the land, the contributions of congestus are lower than those of cumulus (Fig. 5a). Also, the cumulative frequencies (Fig. 5a–d) of the congestus are always higher as compared to cumulus except that over land region during the month of August and September of 2013 (Fig. 5a).

3.3 Longitudinal variation of cloud cells and CTH

Further the longitudinal variation of frequency of occurrence of cloud cells (%) and the corresponding CTH (km) are examined for both the seasons. Also, longitudinal variation of cloud cell (%) and the corresponding CTH (km) are examined at the radar latitude and at latitude ± 1 around the radar latitude. Figure 6 shows the longitudinal variation of frequency of occurrence of number of cloud cells (%) during 2013 and 2014 over sea (Fig. 6a, c, i, k) and land (Fig. 6b, d, m, o) areas by considering all the observations and at radar latitude respectively. The vertical line in each plot indicates the longitude of the location of radar. It is observed here that the frequency (expressed in terms of percentage) is higher over the sea region (Fig. 6a,

c, i, k) as compared to that over the land region (Fig. 6b, d, m, o) during both the years in both cases. Krishnamurti and Ramanathan (1982) reported existence of deep convection offshore of the western coast than that over the adjacent land region during the onset of 1979 monsoon. The frequency of occurrence of cloud cells is higher during the excess monsoon year 2013 as compared to normal monsoon year 2014 over the corresponding sea and land regions. It is clear from Fig. 6a and c that over the sea region the frequency increases initially away from the location of the radar towards the sea and attains maximum at a distance of ~50–60 km from the coast in both the seasons. Grossman and Garcia (1983) reported that persistent deep convection is located off the western coasts of India, and Grossman and Durran (1984) found that offshore convection is the major component of the southwest monsoon circulation in the monsoon season using the 7 years high reflective cloud (HRC) data. Similarly, over the land region (Fig. 6b, d), the frequency increases initially as one moves further inland from the location of the radar and attains maximum ~50–60 km away from the coast. The maximum cloudiness off the coast at a distance of 50–60 km over the AS is consistent with the earlier findings by Krishnamurti and Ramanathan (1982), Grossman and Garcia (1983), and Grossman and Durran (1984). However, another maximum at similar distance from the location of the radar over the land area is the new feature, not noticed before. This may be attributed to Hydraulic Jump phenomenon caused by the interaction between westerly flow, WG, and stability of the atmosphere (Kulkarni et al. 2022).

Figure 6 (e–h and m–p) shows the longitudinal variation of the CTH over sea and land regions in both the monsoon seasons in both the cases. It is seen that the CTH shows inverse variation with the frequency of occurrence of cloud cells. Further, it is evident from this figure that the mode in the frequency of occurrence of cloud cells is associated with the minimum CTH over both sea and land regions during both the monsoon seasons. The location of Mumbai radar is at 72.81° E longitude. Over the land, the maximum CTH occurs at 74.3° E longitude, which is about 150 km away from the coast. The precise location of maximum CTH over AS has been seen at 71.3° E longitude. The maximum CTH over the sea and land are comparable. Similar features are observed when longitudinal variation of frequency of occurrence of cloud cells (%) and maximum cloud top height (km) are examined at latitude ± 1 around the radar latitude. These are shown in Fig. 7(a–p). The location of CTH away from the coast over the land may be due to increasing continental impact on the convection. However, the location of maximum CTH over the AS is further away from the coast than showed in the earlier studies. This is a new feature and requires further studies.

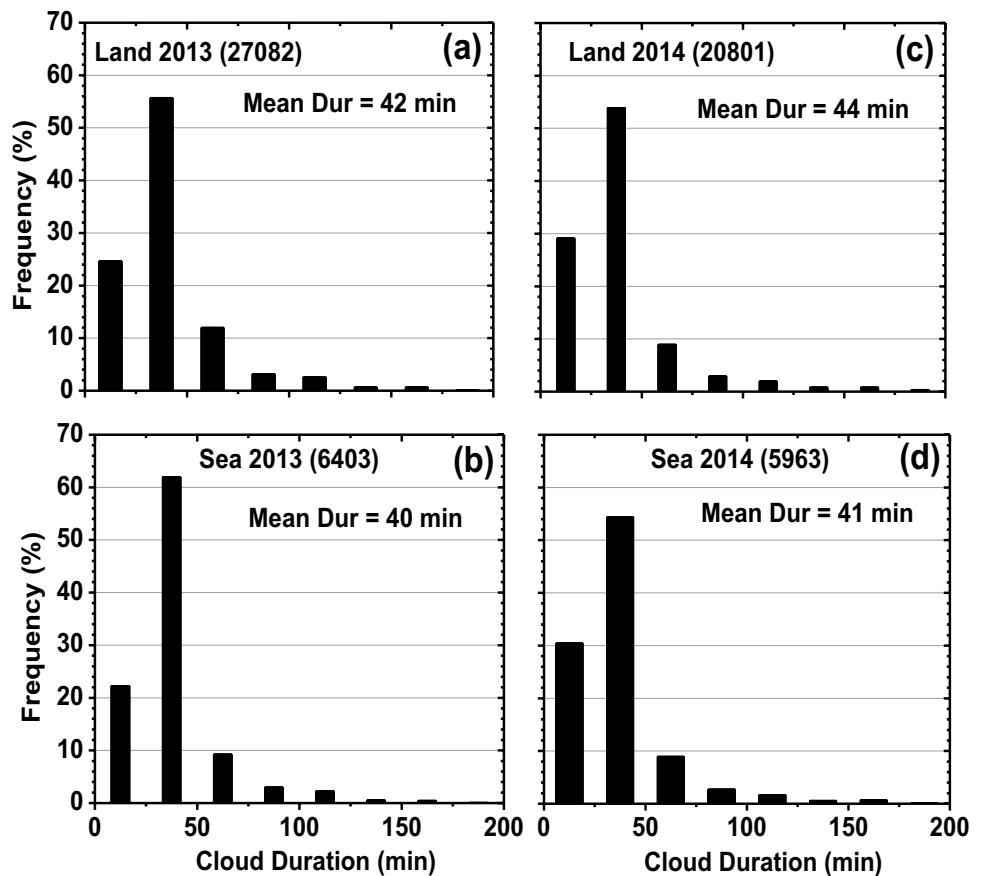
3.4 Diurnal variation of cloud cells

The diurnal variations of convective activity and rainfall greatly influence the energy and water cycles on a daily basis (Ohsawa et al. 2001). The diurnal variation of convection has been studied mainly using the satellite observations and models (Cui 2008; Gray and Jacobsen 1977; Hartmann and Recker 1986; Hendon and Woodberry 1993; Houze et al. 1981; Kubota et al. 2004; Liu and Moncrieff 1998; Meisner and Arkin 1987; Reed and Jaffe 1981). Hendon and Woodberry (1993) reported that over the tropical land mass, the significant diurnal variation of deep convection is observed whereas the diurnal variation over the tropical oceans is weak. Diurnal variation of number of cloud cells (%) during the summer monsoon seasons of 2013 and 2014 over the land and sea regions is shown in Fig. 8a–d. The time scale is in UTC (local time = UTC + 0530 h). The diurnal cycle is broad with maximum between 0800–1200 UTC and minimum around 0300–0600 UTC. This is equivalent to maximum in the early afternoon hours and minimum in the morning hours on the local time scale similar to that reported by earlier studies (Gray and Jacobsen 1977; Hendon and Woodberry 1993; Kubota et al. 2004; Liu and Moncrieff 1998; Ohsawa et al. 2001, Morwal et al. 2016, 2017).

3.5 Distribution of cloud duration

One radar volume scan completes in ~11 min. Therefore, a cell observed at least for two successive volume scans is identified as cloud cell. Hence, the minimum detectable duration of the cloud is ~22 min. Therefore, the interval of 25 min is taken for frequency distribution of cloud duration. The frequency distribution (%) of the cloud duration during the summer monsoon seasons of 2013 and 2014 over the land and sea regions is shown in Fig. 9a–d. The maximum frequency is seen in class interval 25–50 min in all the plots and the mean cloud duration is 40–44 min which is of the same order as observed over Baramati and Shegaon, India regions (48 min) during the summer monsoon season by Morwal et al. (2017). The frequency distribution is positively skewed. There is no variation in frequency distributions of cloud durations during both the years. The mean cloud duration over this region is more as compared to that observed by Lopez (1976) for the cloud population of the tropical disturbances in the Northwest Atlantic (7.6 min) and by Kumar et al. (2013a) for the tropical convective clouds over the Darwin, Australia (modal value < 20 min). The mean cloud duration over this region is lower as compared to that observed over the Mahabubnagar, Hyderabad (55 min) by Morwal et al. (2016) during the withdrawal and post-withdrawal monsoon period, over the GATE region (88 min) by Houze and Cheng (1977) during summer season. It is observed that more than 90% of the cloud cells have short

Fig. 9 Frequency distribution of Cloud duration (%) using radar during the summer monsoon season for 2013 over (a) Land and (b) sea region and 2014 over (c) land and (d) sea region



duration (<75 min). The frequency of the long duration cloud cells is very less (<10%).

3.6 Scale-wise distribution of cloud cells

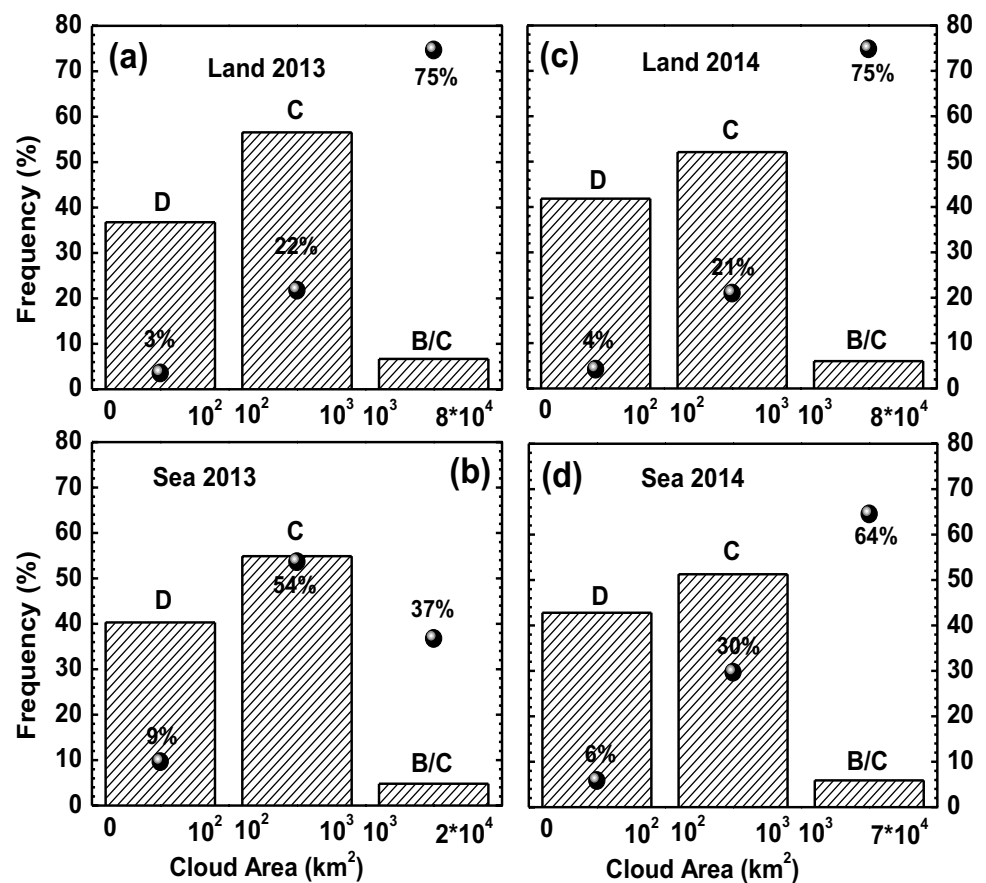
The cloud cells have been categorized into different spatial convection categories based on the horizontal area occupied by the cloud cells. This categorization was used in the past studies by Lo´pez (1976), Houze and Cheng (1977), Cheng and Houze (1979), and Morwal et al. (2016, 2017). These scales have initially been introduced by the Interim Scientific and Management Group (ISMG 1972) and subsequently used by Iwanchuk (1973). These scales are (Morwal et al. 2016): synoptic scale (A: size > 10⁶ km²), cloud cluster scale (B: size 10⁵–10⁶ km²), mesoscale (B/C: size 10³–10⁵ km²), mesoscale (C: size 10²–10³ km²), and cumulus scale (D: size 1–10² km²). Here we have used the same spatial scale and frequencies of occurrences of different scales over land and sea regions during the summer monsoon seasons of 2013 and 2014 and are shown in Fig. 10a–d. It is evident that over the study region we have observed the cells of D, C, and B/C scales. The vertical bars indicate the frequency of occurrence of the scales and solid circles represent the area occupied by the cells in those scales. The frequency of occurrence D, C and B/C scales cells lies in the range

37–43%, 51–57%, and 5–7%, respectively and does not show much variation during the two monsoon seasons or land/sea regions. However, the total area occupied by the D and C scale cells are more over the sea region (6–9% and 30–54%, Fig. 10b, d) as compared to land region (3–4% and 20–21%, Fig. 10a, c). The major area is occupied by the B/C scale cells over the land region (75%) during both the seasons (Fig. 10a, c). Over the sea region, the maximum area is occupied by C scale cells (54%) in the excess monsoon year 2013 (Fig. 10b) and by B/C scale cells (64%) in the normal monsoon year 2014 (Fig. 10d).

The variation of the CTH (km) in the D, C and B/C scale is shown in Fig. 11a–d in both the seasons over the land and sea regions. It is clear from these plots that the CTH showed steady increase from D to B/C scale. The average CTH of D scale cells is ~4.3 km, that of C scale cells is ~5 km and of B/C scale cells is ~8.3 km. The CTH over land/sea regions of all the scales during the excess monsoon year 2013 are lower as compared to corresponding scales in the normal monsoon year 2014. The variation of CTH from D to C scale is less (0.56–0.88 km) but it is more from C to B/C scale (2.15–4.01 km).

The cloud durations (min) in the D, C and B/C scale are shown in Fig. 12a–d for both the seasons and for land and sea regions. It is clearly evident that the cloud duration

Fig. 10 Frequency of occurrence of clouds of scale D, C and B/C during the summer monsoon season for 2013 over (a) land and (b) sea region and 2014 over (c) land and (d) sea region



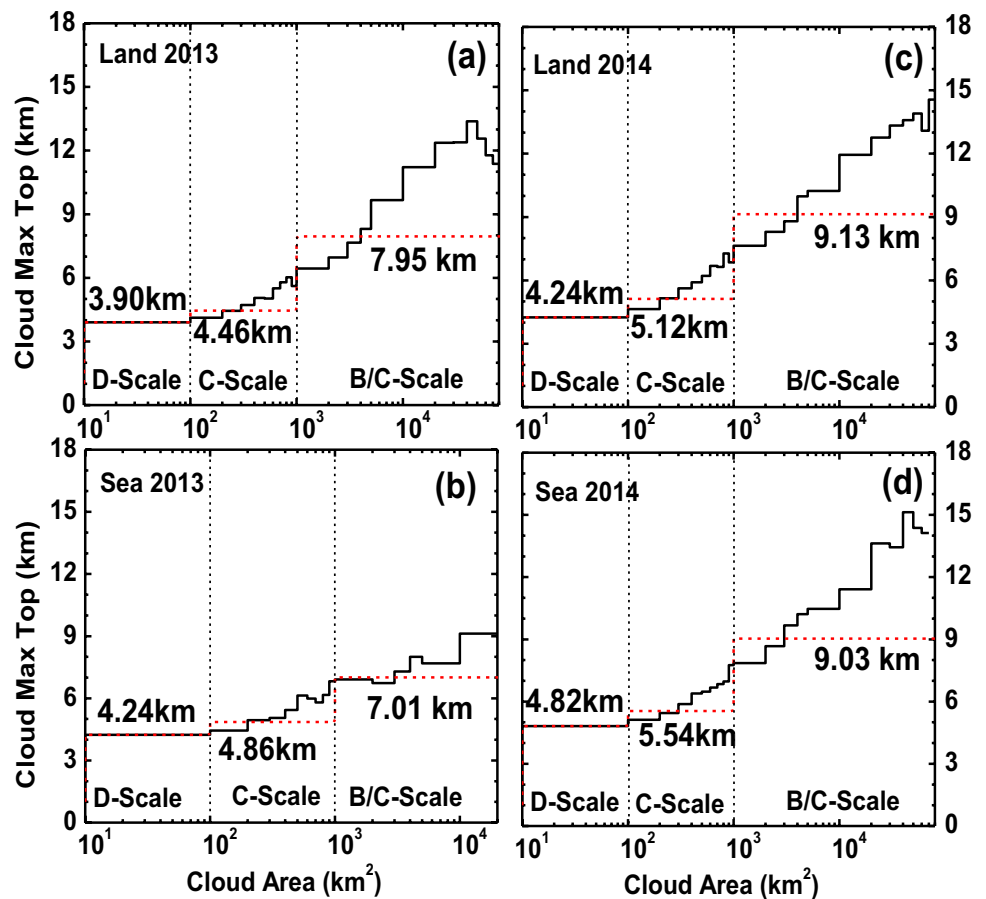
increases continuously from lower scale D to higher scale B/C. The average durations of D (~29 min) and C (~47 min) cells are nearly same over land and sea regions in the both the seasons. However, the duration of B/C scale cells are slightly higher over the land during the year 2014 (Fig. 12c). The mean duration of B/C scale cells is ~86 min. The increase in cell duration from D to C scale is ~17–21 min and that from C to B/C scale is ~31–56 min.

3.7 Height distribution of mesoscale convective systems (MCS) and sub-MCS

There is another way to examine the maximum cloud top heights. The cloud cells can be categorized into two classes based on their horizontal sizes. This approach has been used by Johnson et al. (1999), Rickenbach and Rutledge (1998) and Morwal et al. (2016, 2017). The two categories are mesoscale convective system (MCS) and sub-MCS. The MCS includes the cloud cells with horizontal size $\geq 100 \text{ km}^2$ and the cloud cells with horizontal extent $< 100 \text{ km}^2$ are termed as sub-MCS. They represent the organized convection and isolated convection, respectively. Mesoscale convective systems (MCSs) are the organized convective clouds having characteristic structure with a large cirriform cloud form on the top.

MCS cause contiguous rainfall over 100 km in the horizontal extent, and for a large proportion of precipitation in the tropics (Houze 2004). The frequency distribution of maximum cloud top heights (km) of MCS (green line), sub-MCS (red line), and total cells (black line) during the summer monsoon season of 2013 and 2014 over land and sea regions is shown in Fig. 13a–d. It is seen that the contribution of MCS category is dominated (57–63%). This indicates that the convection is well organized over the coastal regions. This is different than that observed by Johnson et al. (1999) and Rickenbach and Rutledge (1998) over the TOGA COARE region. Also, it is different than that over rain-shadow regions of Hyderabad reported by Morwal et al. (2016) and rain-shadow and drought-hit regions of Baramati and Shegaon, respectively reported by Morwal et al. (2017). All these studies reported the most common occurring category as sub-MCS. Primary peak is observed at maximum cloud top height of 3–4 km for both MCS and sub-MCS categories in all the plots with highest frequency of occurrence for the sub-MCS category. However, during 2013/2014 for both categories, the frequencies are higher over land region (sub-MCS: 58%/49.3%, MCS: 41.6%/27.2%) as compared to sea region (sub-MCS: 52%/39.3%, MCS: 32.9%/19.4%). Another peak with low frequency is observed at 6–7 km height in both MCS and

Fig. 11 Average cloud maximum top heights (CTH, km) in different size bins (black solid line) and average CTH for scales D, C and B/C (red dashed line) during the summer monsoon season for 2013 over (a) land and (b) sea region and 2014 over (c) land and (d) sea region



sub-MCS categories. Here maximum frequency is associated with the MCS category being less over land and more over the sea region.

4 Mechanism of high rainfall over the study region

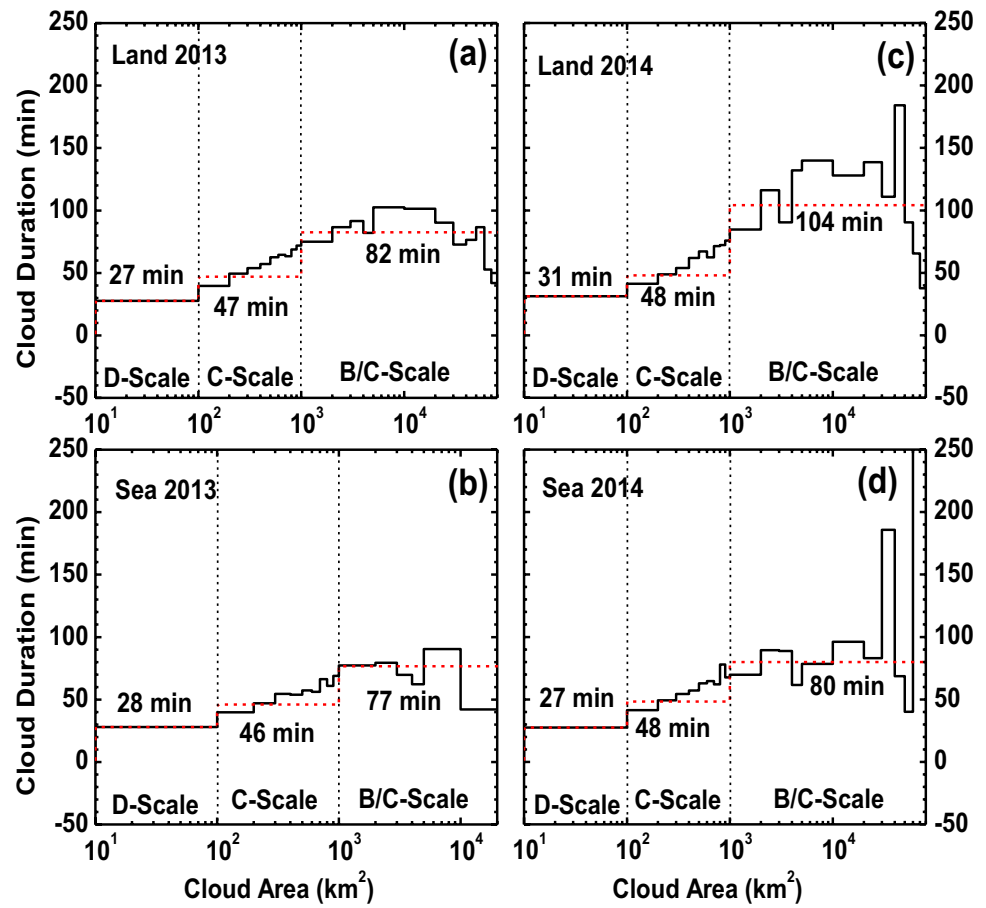
The mechanism of high rainfall emerged from the study is as follows. As the south westerly monsoon winds approach the west coast, they feel the impact of WG in deceleration in the wind speed. The moist convection and hence cloud development start building at a distance of 150 km from the coast. The maximum cloud top heights occur at a distance of 50–60 km from the coast over the sea. Study by Mahes Kumar et al. (2014) showed the existence of low vertical velocities over the AS in the monsoon season. The mean height of the clouds in the range 4.44–5.29 km found in this study using radar data is consistent with Mahes Kumar et al. (2014). The broad diurnal cycle over the sea and land is indicative of persistence of convection over the study area. In the presence of convergence over the sea area, with the availability of moisture, there is a continuous production of MCS over the sea which is transported over the adjacent land

area. The integrated effect of all these factors is to produce high rainfall over the coast and the adjacent land region. All these fine structures of cloud distributions vary with the large-scale background setting which intensifies interannually in the excess monsoon season and intraseasonally in the active monsoon conditions.

5 Conclusions

Clouds are the visible form of moist convection. Spatio-temporal distribution of the convection over the west coast of India and adjacent AS has been important to understand the rainfall distribution. Previous studies regarding this feature have been carried out using satellite data for limited periods. The present study for the first time utilizes the ground-based S-band radar data for understanding the spatio-temporal variability of cloud cells in the area within 150 km from the location of the radar. The location of Mumbai radar is on the west coast of India. The area spanned by the radar covers both sea and land regions. This gives an opportunity to study the cloud characteristics over sea and land simultaneously. The study has been carried out for two monsoon seasons viz. 2013 and 2014. The season 2013 was in the excess and 2014

Fig. 12 Average cloud duration (minutes) in different size bins (black solid line) and average cloud duration for scales D, C and B/C (red dashed line) during the summer monsoon season for 2013 over (a) land and (b) sea region and 2014 over (c) land and (d) sea region

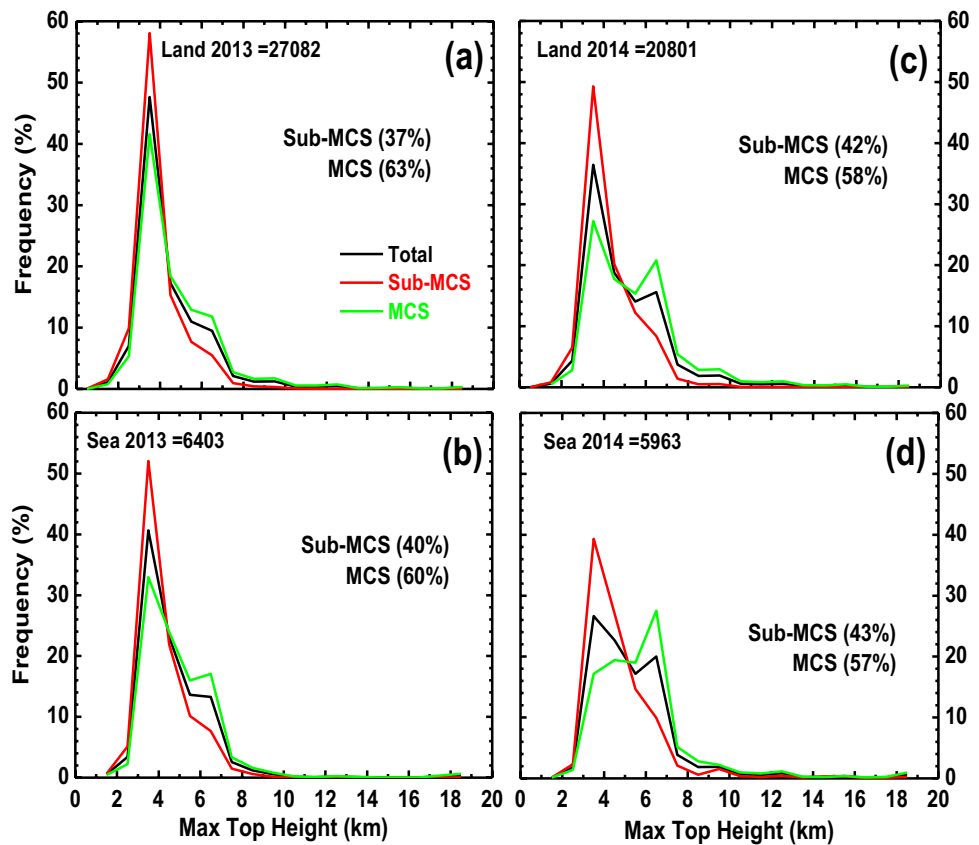


was in the normal monsoon rainfall categories. Within the seasons, there were periods of high and low rainfalls. The cloud characteristics brought out in the paper pertain to both the intraseasonal and interannual monsoon variabilities. The total number of cloud cells were higher in the 2013 season than that in the 2014 season indicating that the large-scale circulation is the driving mechanism for the development of convection over the study area. In both seasons, the total number of cloud cells were nearly 4 times higher over the land area than that over the sea area. This suggests that the land surface processes play a crucial role in enhancing the convection over the land area. The cloud parameter CTH is closely linked with the intensity of the convection. The mean CTH is found to lie between 4.49 km and 5.44 km. There is no statistically significant difference between CTH over the sea and land. Both these factors are consistent with the findings of Padmakumari et al. (2018) that the clouds over the peninsular Indian region are of gray-ocean type. Thus, the convection over the study area has remarkable marine characteristics. The land surface is wet due to high and persistent rainfall throughout the monsoon season, and the distance traveled by the clouds over the land after forming over the sea is not very large; both of these contribute to the clouds to retain marine characteristics.

Among the three cloud types, congestus is found to be the major contributor to the total cloud population. The frequency of deep convective clouds is very low which is consistent with the findings of Houze et al. (2007). Earlier studies based on the satellite data showed that there exists a zone of convergence and hence an area of convection at a distance of 50–60 km of the west coast over the sea. This study has brought out the detailed structure of the convection over the sea and land. The area of maximum cloudiness lies at distance of 50–60 km on both sides of the radar location. The area of maximum convergence over the sea is consistent with the previous studies; however, this study has brought out that there exists another area at a similar distance over the land also. This has been speculated due to “Hydraulic Jump” associated with the interaction of westerly flow with the west coast mountains in the thermodynamic stable setting (Kulkarni et al., 2022). When the clouds are classified into MCS and sub-MCS categories, this study shows that the MCS category contributes significantly to the total cloud population.

The diurnal cycle of the number of cloud cells is broad with a maximum between 0800–1200 UTC and a minimum around 0300–0600 UTC. This is equivalent to a maximum in the early afternoon hours and a minimum in the morning

Fig. 13 Frequency distribution of maximum cloud top heights (CTH) of the total (black line), mesoscale convective clouds (MCS, green line), and Sub-MCS (red line) during the summer monsoon season of 2013 over (a) land and (b) sea region and 2014 over (c) land and (d) sea region



hours on the local time scale. The mean cloud duration is 40–44 min. The categorization of cloud cells based on the horizontal area (scale-wise distribution) showed that the major contribution to total cloud cells is by the B/C scale cells over the land and is by C scale cells over the sea.

The study has brought out the mechanism of high rainfall over the west coast and adjacent land regions. The variability of cloud features brought out in this study will help to understand its wider role in monsoon circulation over India besides high rainfall activity over the west coast and adjacent land area.

Acknowledgements IITM is fully supported by the Ministry of Earth Sciences (MoES), Govt. of India, New Delhi. The authors would like to thank India Meteorological Department (IMD) for radar data and high resolution gridded rainfall data sets used in this study.

Author contribution The authors have contributed as follows. Morwal Savita B: experiment designing, data analysis, first draft writing; Padmakumari B: data preparation, interpretation, manuscript editing and reviewing; Hosalikar K.S. and Sai Krishnan K.C.: radar data source, manuscript editing and reviewing; Maheskumar R.S., Narkhedkar S.G., and Pandithurai G.: manuscript editing and reviewing; Kulkarni J. R.: original concept, first draft writing and supervision of the work. All the authors have discussed the results and contributed to the final manuscript.

Funding IITM is funded by the Ministry of Earth Sciences (MoES), Govt. of India, New Delhi.

Data availability The radar data and high resolution gridded rainfall data are available from India Meteorological Department (IMD) upon reasonable request.

Code availability TITAN software used for radar data analysis is freely available.

Declarations

Ethics approval The manuscript has not been submitted to more than one journal for simultaneous consideration. The manuscript has not been published elsewhere previously.

Consent to participate Not applicable.

Consent for publication Not applicable.

Conflict of interest The authors declare no competing interests.

References

Bhat GS, Kumar S (2015) Vertical structure of cumulonimbus towers and intense convective clouds over the South Asian region during the summer monsoon season. *J Geophys Res* 120:1710–1722. <https://doi.org/10.1002/2014JD022552>
 Braham RR Jr (1958) Cumulus cloud precipitation as revealed by radar-Arizona 1955. *J Meteorol* 15:75–83

- Cheng C, Houze RA Jr (1979) The distribution of convective and mesoscale precipitation in GATE radar echo patterns. *Mon Wea Rev* 107:1370–1381
- Cui X (2008) A cloud-resolving modeling study of diurnal variations of tropical convective and stratiform rainfall. *J Geophys Res* 113:D02113. <https://doi.org/10.1029/2007JD008990>
- DeMott CA, Rutledge SA (1998) The vertical structure of TOGA COARE Convection. Part I: Radar Echo distributions. *J Atmos Sci* 55:2730–2747
- Dixon M, Wiener G (1993) TITAN: Thunderstorm Identification Tracking, Analysis and Nowcasting – a radar based methodology. *J Atmos Oce Tech* 10:785–796
- Donaldson R (1964) A demonstration of antenna beam errors in radar reflectivity patterns. *J Appl Meteorol* 3:611–623
- Francis PA, Gadgil S (2006) Intense rainfall events over the west coast of India. *Meteorol Atmos Phys* 94:27–42
- Goudenhoofd E, Reyniers M, Delobbe L (2010) Long term analysis of convective storm tracks based on C-band radar reflectivity measurements. Proc. Sixth European Conf. on Radar in Meteorol and Hydrol, Sibiu, Romania, National Meteorol Admin, 1–7
- Gray WM, Jacobsen RW (1977) Diurnal variation of deep cumulus convection. *Mon Wea Rev* 105:1171–1188
- Grossman RL, Garcia O (1983) A seven year distribution of monsoon convective cloud and its variability. Proc. 7th Conf. Climate Diagnostics (Boulder, Oct. 1982). NOAA/Climate Analysis Center, 172–179
- Grossman RL, Durran DR (1984) Interaction of low-level flow with the Western Ghat mountains and offshore convection in the summer monsoon. *Mon Wea Rev* 112:652–672
- Hartmann DL, Recker EE (1986) Diurnal variation of outgoing radiation in the tropics. *J Clim* 25:800–812
- Hendon HH, Woodberry K (1993) The diurnal cycle of tropical convection. *J Geophys Res* 98:16623–16637
- Houze RA Jr (1997) Stratiform precipitation in regions of convection: a meteorological paradox? *Bull Amer Meteor Soc* 78:2179–2196
- Houze RA Jr (2004) Mesoscale convective systems. *Rev Geophys* 42:43. <https://doi.org/10.1029/2004RG000150>
- Houze RA Jr (2012) Orographic effects on precipitating clouds. *Rev Geophys* 50:RG1001-47. <https://doi.org/10.1029/2011RG000365>
- Houze RA Jr, Cheng CP (1977) Radar characteristics of tropical convection observed during GATE: mean properties and trends over the summer season. *Mon Wea Rev* 105:964–980
- Houze RA Jr, Geotis SG, Marks FD Jr, West AK (1981) Winter monsoon convection in the vicinity of North Borneo, I, Structure and time variation of clouds and precipitation. *Mon Wea Rev* 109:1595–1614
- Houze RA Jr, Wilton DC, Smull BF (2007) Monsoon convection in the Himalayan region as seen by the TRMM precipitation radar. *Q J R Meteor Soc* 133:1389–1411
- ISMG (Interim Scientific and Management Group) (1972) Experiment design proposal for the GARP Atlantic Tropical Experiment. GATE Rep. No. 1, WMO ICSU, Geneva. Pp 188
- Iwanchuk RM (1973) Characteristics and distribution of precipitation areas over the tropical Atlantic. M S Thesis, Dept of Meteorology, MIT, Cambridge, Mass. Pp 106
- Johnson RH, Rickenbach TM, Rutledge SA, Ciesielski PE, Schubert WH (1999) Trimodal characteristics of tropical convection. *J Climate* 12:2397–2417
- Kokhanovsky AA, Vountas M, Rozanov VV, Lotz W, Bovensmann H, Burrows JP, Schumann U (2007) Global cloud top height and thermodynamic phase distribution as obtained by SCIAMACHY on ENVISAT. *Int J Remote Sens* 28:4499–4507
- Kothawale DR, Rajeevan M (2017) Monthly, seasonal and annual rainfall time series for all-India, homogeneous regions and meteorological subdivisions: 1871–2016, August 2017, Indian Institute of Tropical Meteorology Research Report No. RR-138. <https://www.tropmet.res.in/Research%20Report-136-Page>
- Krishnamurti TN, Ramanathan Y (1982) Sensitivity of the monsoon onset to differential heating. *J Atmos Sci* 39:1290–1306
- Kubota H, Numaguti A, Emori S (2004) Numerical experiments examining the mechanism of diurnal variation of tropical convection. *J Meteor Soc Japan* 82:1245–1260
- Kulkarni J, Deshpande N, Morwal SB, Kothawale DR, Narkhedkar SG, Kumar V (2022) Hydraulic jump: the cause of heavy rainfall on the immediate lee side of the Western Ghats in the Maharashtra state of India. *Int J Climatol*. 1–14. <https://doi.org/10.1002/joc.7658>
- Kumar S (2016) Three dimensional characteristics of precipitating cloud systems observed during Indian summer monsoon season. *Adv Space Res* 58:1017–1032
- Kumar S (2017) A ten-year climatology of vertical properties of moist active convective clouds using Indian region using TRMM PR. *Theor App Climatol* 127:429–440
- Kumar S, Bhat GS (2017) Vertical structure of orographic precipitating clouds observed over south Asia during summer monsoon season. *J EarthSys Sci* 126(114):1–14
- Kumar VV, Protat A, May PT, Jakob C, Penide G, Kumar S, Davies L (2013) On the effects of large-scale environment and surface types on convective cloud characteristics over Darwin, Australia. *Mon Wea Rev* 141:1358–1374
- Kumar VV, Jakob C, Protat A, May PT, Davies L (2013) The four cumulus cloud modes and their progression during rainfall events: a C-band polarimetric radar perspective. *J Geophys Res* 118:8375–8389. <https://doi.org/10.1002/jgrd.50640>
- Liu C, Moncrieff MW (1998) A numerical study of the diurnal cycle of tropical oceanic convection. *J Atmos Sci* 55:2329–2344
- Lo'pez RE (1976) Radar characteristics of cloud populations of tropical disturbances in the 769 northwest Atlantic. *Mon Wea Rev* 104:268–283
- Lo'pez RE (1977) The lognormal distribution and cumulus cloud populations. *Mon Wea Rev* 105:865–872
- Maheskumar RS, Narkhedkar SG, Morwal SB, Padmakumari B, Kothawale DR, Joshi RR, Deshpande CG, Bhalwankar RV, Kulkarni JR (2014) Mechanism of high rainfall over the Indian west coast region during the monsoon season. *Cli Dyn* 43:1513–1529
- May PT, Ballinger A (2007) The statistical characteristics of convective cells in a monsoon regime (Darwin, Northern Australia). *Mon Wea Rev* 138:55–73
- Medina S, Houze RA Jr, Kumar A, Niyogi D (2010) Summer monsoon convection in the Himalayan region: Terrain and land convection. *Q J R Meteor Soc* 136:593–616
- Meisner BN, Arkin PA (1987) Spatial and annual variations in the diurnal cycle of large-scale tropical convective cloudiness and precipitation. *Mon Wea Rev* 115:2009–2032
- Morwal SB, Narkhedkar SG, Padmakumari B, Maheskumar RS, Kothawale DR, Dani KK, Burger R, Bruintjes RT, Kulkarni JR (2016) Cloud characteristics over the rain-shadow region of North Central peninsular India during monsoon withdrawal and post-withdrawal periods. *Clim Dyn* 46(1):495–514. <https://doi.org/10.1007/s00382-015-2595-0>
- Morwal SB, Narkhedkar SG, Padmakumari B, Maheskumar RS, Kulkarni JR (2017) Characteristics of precipitating monsoon convective clouds over rain-shadow and drought-hit regions of India using radar. *Clim Dyn* 50:3571–3594. <https://doi.org/10.1007/s00382-017-3826-3>
- Ohsawa T, Ueda H, Hayashi T, Watanabe A, Matsumoto J (2001) Diurnal variations of convective activity and rainfall in tropical asia. *J Meteor Soc Japan* 79:333–352
- Osuri KK, Mohanty U, Routray A, Niyogi D (2015) Improved prediction of Bay of Bengal Tropical cyclones through

- assimilation of doppler weather radar observations. *Mon Wea Rev* 143:4533–4560
- Padmakumari B, Maheskumar RS, Harikishan G, Morwal SB, Kulkarni JR (2018) Rain-shadow: An area harboring “Gray Ocean” clouds. *Atmos Res* 205:70–79
- Parthasarathy B, Munot AA, Kothawale DR (1995) Monthly and seasonal rainfall series for All-India homogeneous regions and meteorological subdivisions: 1971–1994. Contributions from Indian Institute of Tropical Meteorology, Research Report RR-065.
- Rao YP (1976) Southwest Monsoon, India Meteorological Department, Meteorological Monograph No 1/1976, p 367
- Reed RJ, Jaffe KD (1981) Diurnal variation of summer convection over West Africa and the tropical eastern Atlantic during 1974 and 1978. *Mon Wea Rev* 109:2527–2534
- Rickenbach TM, Rutledge SA (1998) Convection in TOGA COARE: horizontal scale, morphology, and rainfall production. *J Atmos Sci* 55:2715–2729
- Roca R, Ramanathan V (2000) Scale dependence of monsoonal convective systems over the Indian Ocean. *J Clim* 13:1286–1298
- Romatschke U, Houze RA Jr (2011) Characteristics of precipitating convective systems in the south Asian monsoon. *J Hydrometeor* 12:3–25
- Romatschke U, Medina S, Houze RA Jr (2010) Regional, seasonal, and diurnal variations of extreme convection in the south Asian region. *J Climate* 23:419–439
- Sindhu KD, Bhat GS (2018) Characteristics of monsoonal precipitating cloud systems over the Indian subcontinent derived from weather radar data. *Quart Roy Met Soc* 144:1742–1760
- Sindhu KD, Bhat GS (2021) Seasonal characteristics of storms over the Indian subcontinent. *Nat Sci Rep* 11:3355. <https://doi.org/10.1038/s441598-021/82237-w>
- Weather in India (2014) Monsoon Season (June–September 2013). *Mausam* 65:441–460
- Weather in India (2015) Monsoon Season (June–September 2014). *Mausam* 66:657–674
- Publisher's note** Springer Nature remains neutral with regard to jurisdictional claims in published maps and institutional affiliations.
- Springer Nature or its licensor holds exclusive rights to this article under a publishing agreement with the author(s) or other rightsholder(s); author self-archiving of the accepted manuscript version of this article is solely governed by the terms of such publishing agreement and applicable law.